

Dynamics of a two-state quantum dot laser with saturable absorber

E. A. Viktorov

Optique Nonlinéaire Théorique, Université Libre de Bruxelles, Campus Plaine CP 231, B-1050 Bruxelles, Belgium

M. A. Cataluna, L. O'Faolain, T. F. Krauss, and W. Sibbett

School of Physics and Astronomy, University of St. Andrews, North Haugh, St. Andrews, Fife KY16 9SS United Kingdom

E. U. Rafailov

Carnegie Laboratory of Physics, Division of Electronic Engineering and Physics, University of Dundee, Dundee, DD1 4HN United Kingdom

Paul Mandel^{a)}

Optique Nonlinéaire Théorique, Université Libre de Bruxelles, Campus Plaine CP 231, B-1050 Bruxelles, Belgium

(Received 30 November 2006; accepted 13 February 2007; published online 21 March 2007)

The authors study the regime of self-pulsations in a two-state quantum dot laser with saturable absorber. Experiments demonstrate and theory explains the appearance of self-pulsations at low relaxation oscillation frequency. The system exhibits a period doubling sequence of bifurcations leading to chaos. © 2007 American Institute of Physics. [DOI: 10.1063/1.2715023]

Recent developments in quantum dot (QD) semiconductor lasers have attracted much attention due to their high gain characteristics, low chirp, low feedback, and temperature resilience.¹ The possibility of simultaneous lasing at both the ground state (GS) and excited state (ES) in QD lasers² offers a switching possibility between two distant wavelengths. The first optically gain-switched QD laser operating at both GS and ES was demonstrated in Ref. 3 and stable mode locking via either GS or ES transitions was achieved in Ref. 4.

The dynamics of lasers containing an intracavity saturable absorber has been extensively studied during the last decade (see Ref. 5 and references therein). In QD lasers operating at the GS, self-pulsating regimes were reported in Refs. 6 and 7. In this letter, we report on experimental and theoretical investigations of self-pulsation regimes in a two-section QD laser operating simultaneously on the GS and ES transitions. We show that the competition between the two states results in antiphase dynamics. We also found a period doubling sequence leading to deterministic chaos.

The QD laser used in this work is a two-section device with a total length of 1.3 mm (saturable absorber length is 0.16 mm). The fabrication method is the same as that used in Ref. 8. The active region was grown by molecular beam epitaxy on a GaAs (100) substrate, containing ten self-organized QD layers (grown by NL Nanosemiconductor). Both facets were as cleaved. The device was mounted *p*-side up on a copper heat sink, and a Peltier cooler was used to control the operating temperature (20 °C). The gain section of the laser was electrically pumped by constant bias, and the laser exhibited relatively high average output power, of up to 25 mW in mode-locked operation. The short cavity length was important to achieve simultaneous laser emission in both ground and excited states. By increasing the current in the gain section, the GS gain saturated and lasing appeared for the ES transitions, for a constant value of reverse bias. On the other hand, it was also possible to obtain ES emission if the current in the gain section was kept at a high value, and

the reverse bias was increased in the absorber section (and thus increasing the overall losses in the laser cavity).

The evolution of the optical spectra (Fig. 1) and the frequency of oscillation (Fig. 2) with increasing reverse bias at constant current of 300 mA illustrate (i) the appearance of simultaneous lasing above 1.5 V and (ii) the decreasing frequency of self-pulsations and the sequence of period doubling bifurcations ending with chaos. Two important frequencies are evidenced in Fig. 2: the relaxation oscillation frequency $\nu_r \approx 2.5$ GHz and the self-pulsation frequency which appear at $\nu_a \approx 700$ MHz. As evidenced in the graph, the self-pulsation frequency ν_a decreases with increasing the reverse bias applied in the absorber section, at a constant current injection in the gain section. This fundamentally differs from the well-known phenomena of self-pulsation and *Q*-switched mode locking where the converse occurs. In addition, the pulsations in the GS and ES regimes are phase shifted by about $\pi/2$, indicating an antiphase dynamics similar to that reported for a two-state QD laser with optical feedback.⁹

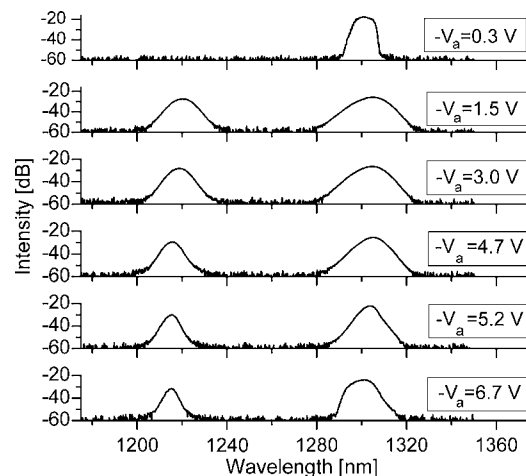


FIG. 1. Experimental results. Evolution of the optical spectrum with increasing reverse bias in the saturable absorber section, while keeping a constant current of 300 mA in the gain section.

^{a)}Electronic mail: pmandel@ulb.ac.be

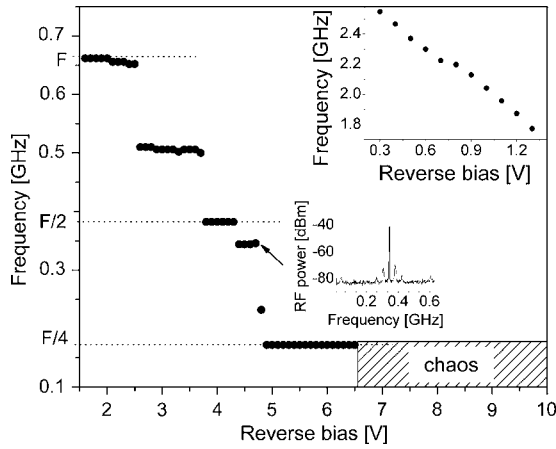


FIG. 2. Experimental results. Evolution of the pulsation frequency with increasing reverse bias in the saturable absorber section, while keeping a constant current of 300 mA in the gain section. The inset demonstrates the evolution of the frequency when the output at the GS is dominant.

The subharmonic sequence in Fig. 2 is not a perfect period doubling route to chaos. Although the first frequencies of the sequence $F \approx 700$ MHz, $F/2 \approx 350$ MHz, and $F/4 \approx 175$ MHz are clearly present, there are two types of additions: (1) discrete small step decrease of F and (more pronounced) $F/2$ and (2) an extra frequency at ≈ 500 MHz. The discrete change in the frequency corresponds to the appearance of side modes as shown in the inset. The low frequency beating is in the range of the multimode frequency fluctuations.¹⁰ The extra frequency indicates that the system has more nonlinearities than those required to generate a Feigenbaum sequence.

In order to account for the observed phenomena, let us consider a QD laser consisting of two sections: a saturable absorber and a gain section, as in the experiment. The equations describing the evolution of the intensities are

$$\dot{I}_g = [2g_g[2\rho_g(t) - 1] - 2g_a[2\rho_{ga}(t) - 1] - 1]I_g, \quad (1)$$

$$\dot{I}_e = [4g_g[2\rho_e(t) - 1] - 4g_a[2\rho_{ea}(t) - 1] - 1]I_e, \quad (2)$$

where $I_{g,e}(t)$ are the normalized intensities of the GS and ES electric fields. The indices g and e refer to the ground and the excited levels. The variables $\rho_{g,e}(t)$ and $\rho_{ga,ea}(t)$ describe the occupation probabilities in a dot located either in the gain or absorber section, respectively. The $g_{g,a}$ are the effective gain factors scaled to the cavity losses. For simplicity, we assume these gain factors to be identical for both GS and ES.

The equations for the occupation probabilities in the amplifying and absorbing sections can be written in the form

$$\partial_t \rho_{g,ga} = -\gamma_{g,ga} \rho_{g,ga} + 2F_{ge}(\rho_{g,ga}, \rho_{e,ea}) - g_{g,a}[2\rho_{g,ga}(t) - 1]I_g, \quad (3)$$

$$\begin{aligned} \partial_t \rho_{e,ea} = & -\gamma_{e,ea} \rho_{e,ea} - F_{ge}(\rho_{g,ga}, \rho_{e,ea}) + F_{we}(\rho_{e,ea}, N_{g,a}) \\ & - g_{g,a}[2\rho_{e,ea}(t) - 1]I_e, \end{aligned} \quad (4)$$

$$\partial_t N_{g,a} = N_{g0,a0} - \Gamma_{g,a} N_{g,a} - 4F_{we}(\rho_{e,ea}, N_{g,a}). \quad (5)$$

The variables $N_{g,a}(t)$ describe the carrier densities in the wetting layers, scaled to the QD carrier density. The parameters $\Gamma_{g,a}$, $\gamma_{g,ga}$, and $\gamma_{e,ea}$ are, respectively, the carrier relaxation rate in the wetting layers and the carrier relaxation rates in

the dots. The dimensionless parameters N_{g0} and N_{a0} describe pumping processes in the gain and the absorber sections. The coefficients 2 and 4 in Eqs. (1)–(5) account for the twofold and fourfold degeneracies of the ground and excited states, respectively.

The functions $F_{we}(\rho_{e,ea}, N_{g,a})$ describe the carrier exchange rate between the wetting layers and the dots. In the most general form, the carrier exchange can be written as

$$F_{we}(\rho_{e,ea}, N_{g,a}) = \tilde{B}_{g,a} N_{g,a} (1 - \rho_{e,ea}) - R_{g,a}^{\text{esc}} \rho_{g,a}, \quad (6)$$

where $1 - \rho_{e,ea}$ is the Pauli blocking factor, $\tilde{B}_{g,a} N_{g,a}$ describes the carrier capture from the wetting layer to the dots with rate $\tilde{B}_{g,a}$, and $R_{g,a}^{\text{esc}}$ is a temperature-dependent coefficient related to the carrier escape from the dots to the wetting layer.

The functions $F_{ge}(\rho_{g,ga}, \rho_{e,ea})$ describe the carrier exchange between the GS and the ES as follows:¹¹

$$F_{ge}(\rho_{g,ga}, \rho_{e,ea}) = B_{g,a} \rho_{e,ea} (1 - \rho_{g,ga}) - C_{g,a} \rho_{g,ga} (1 - \rho_{e,ea}), \quad (7)$$

where the nonradiative decays¹² from the ES to the GS are represented by the rates $B_{g,a}$. The escape processes from the GS to the ES are determined by the rates $C_g = B_g \exp(-\Delta E/k_B T)$, where ΔE represents the positive energy separation between the excited and the ground state levels, k_B is the Boltzmann constant, and T the plasma temperature.

Modeling the processes in the absorber has been less investigated. We consider the most important case: the capture is either much faster than the escape ($B_g \gg C_g$ and $\tilde{B}_g > R_g^{\text{esc}}$) in the gain section or it is slower than the escape ($B_a < C_a$ and $\tilde{B}_a < R_a^{\text{esc}}$) in the absorber section to which the quasiequilibrium conditions cannot be applied.

Together with Eqs. (1)–(5), Eqs. (6) and (7) constitute a closed set of equations. The purpose of this description is not to model a specific laser configuration, but to describe generic properties of the pulsation regime in quantum dot lasers simultaneously operating at the ground and the excited states. Therefore, some of the parameters are selected in order to match the self-pulsation regime. Carrier capture times in the dots have been reported in the literature to be from 1 to 100 ps. We consider capture rates in the gain section $B_g = \tilde{B}_g = 1$, which correspond to 10 ps and assume $R_g^{\text{esc}} = 0.1 \ll \tilde{B}_g$. For the absorber section, we take $\tilde{B}_a = 0.1$, $B_a = 0.35$, and $R_a^{\text{esc}} = 0.5 > \tilde{B}_a, B_a$. The other parameters are typical for QD materials and geometry: $g_g = g_a = 0.9$; $\gamma_{g,ga} = \gamma_{e,ea} = \Gamma_g = \Gamma_a = 0.01$. We used $\Delta E = 55$ meV at room temperature ($k_B T = 25$ meV) to determine C_g . The time t is normalized to $\tau_p = 10$ ps, where τ_p is the photon lifetime.

There are two scenarios for the appearance of instabilities, depending on whether $I_g \approx I_e$ or $I_g \gg I_e$. In both cases, the linear stability analysis shows the existence of two relaxation oscillation frequencies ω_r and $\omega_a < \omega_r$. The frequency ω_r is a relaxation oscillation frequency resulting from the field-matter interaction, and the frequency ω_a results from the coupling/competition between the GS and ES and is known as the low or antiphase relaxation oscillation frequency.⁵

In the first case, both GS and ES are simultaneously excited in the steady state with nearly identical intensities and the coupling between the two states is strong. The pulsations appear via a Hopf bifurcation with the antiphase relaxation oscillation ω_a , and the phase shift between the fluctuations is π .

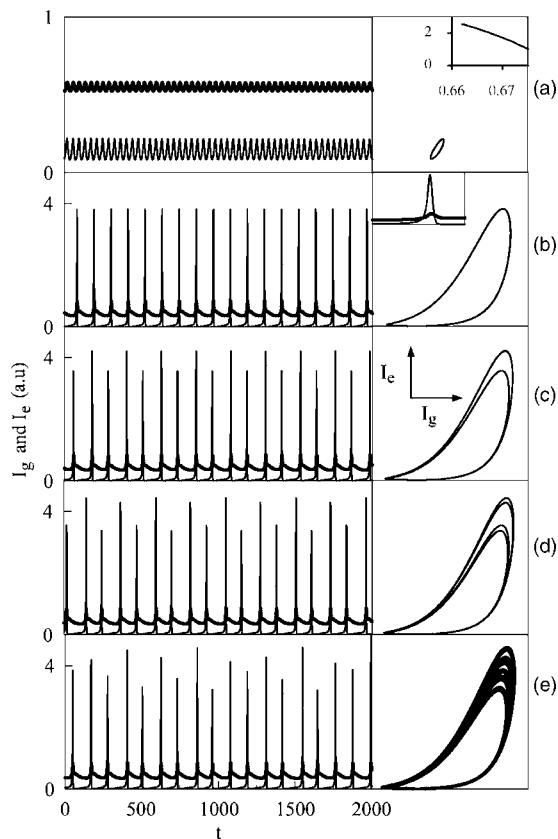


FIG. 3. Numerical simulations. Intensity time traces and corresponding phase portraits for increasing reverse bias: (a) $N_{a0}=0.6615$, (b) $N_{a0}=0.676$, (c) $N_{a0}=0.6762$, (d) $N_{a0}=0.6763$, and (e) $N_{a0}=0.67635$. The time traces demonstrate (i) decreasing frequency of oscillations and (ii) the period doubling route to chaos. The inset in (a) shows the evolution of the frequency of pulsations in gigahertz with increasing N_{a0} when the GS output is dominant. The inset in (b) illustrates the phase shift between the GS (bold) and ES pulsations. The vertical axis of the phase portrait in (a) was multiplied by 5.

tuations at the GS and ES is about $\pi/2$ at the bifurcation point. The laser output evolves towards chaos via a sequence of period doubling bifurcations.

The second case corresponds to the experimental observations. Let us fix the pumping rate in the gain section $N_{g0}=1.25$ and follow the dynamics by changing the reverse bias N_{a0} . The results are shown in Fig. 3. For $N_{a0}=0.66$ (not shown on the figure) both GS and ES are simultaneously in steady state. The GS intensity is dominant, $I_g \gg I_e$, and the coupling between the GS and ES is weak. The linear stability analysis shows the existence of two relaxation oscillation frequencies $\omega_r \approx 0.16$ and $\omega_a \approx 0.04$. The ratio $\omega_a/\omega_r \approx 1/4$ between these frequencies is very close to the experimental measurements. Both frequencies decrease fast with the increase of the reverse bias N_{a0} . The weak coupling between I_g and I_e in steady state changes the frequency at the bifurcation. The pulsations appear at $N_{a0}=0.6615$ via a Hopf bifurcation with the fundamental relaxation oscillation ω_r and no phase shift between the pulsations. Increasing N_{a0} leads to a significant variation of the pulsations and a fast decrease of their frequency. Similar to the experiment, a phase shift appears between the pulsations at the GS and ES as shown in the inset. Further increasing N_{a0} leads to a sequence of

period doubling bifurcations ($N_{a0}=0.6762$) and chaos ($N_{a0}=0.67635$) in full agreement with the experiment.

The intensity time traces shown in Fig. 3 also display the difference between the pulsations in the GS and the ES. The pulsations in the ES have a smaller width and larger amplitude. The relative smallness of the ES-related pulse width was already reported.³ The difference between the intensity pulsations corresponds to the difference between the occupation probabilities in the GS and ES. It is related to the carrier exchange between the GS and ES, described in our model by the function $F_{ge}(\rho_{g,ga}, \rho_{e,ea})$. The coupling between the GS and ES is not symmetric due to the asymmetries in the capture/escape processes. It results in the different pulsation amplitudes and profiles displayed in Fig. 3, so that the pulses are no longer in phase due to phase-amplitude coupling.

In conclusion, we studied the regime of self-pulsations in a two-state quantum dot laser with saturable absorber. There is a good correspondence between the experiment and the model which predicts the appearance of antiphase self-pulsations in the low frequency range. The pulsation frequency decreases with increasing reverse bias. The system exhibits a period doubling sequence of bifurcations and chaos.

Note added in proof. After submission of this letter, a self-pulsating regime involving both ground and excited states was also reported.¹³

Two of the authors (E.A.V. and P.M.) acknowledge support of the Fonds National de la Recherche Scientifique (Belgium) and the Interuniversity Attraction Pole Programme-Belgian Science Policy. Four of the authors (M.A.C., L.O., T.F.K., and W.S.) acknowledge the financial support from EPSRC, through the Ultrafast Photonics Collaboration. The work of one of the authors (M.A.C.) was supported by Fundação para a Ciência e Tecnologia, Portugal, through a graduate scholarship award. The work of L.O.F. was supported by the ePIXnet Network of Excellence.

¹D. Bimberg, M. Grundmann, and N. N. Ledentsov, *Quantum Dot Heterostructures* (Wiley, New York, 1999).

²A. Markus, J. X. Chen, C. Paranthoen, A. Fiore, C. Platz, and O. Gauthier-Lafaye, *Appl. Phys. Lett.* **82**, 1818 (2003).

³E. U. Rafailov, A. D. McRobbie, M. A. Cataluna, L. O'Faolain, W. Sibbett, and D. A. Livshits, *Appl. Phys. Lett.* **88**, 041101 (2006).

⁴M. A. Cataluna, W. Sibbett, D. A. Livshits, J. Weimert, A. R. Kovsh, and E. U. Rafailov, *Appl. Phys. Lett.* **89**, 081124 (2006).

⁵P. Mandel, *Theoretical Problems in Cavity Nonlinear Optics* (Cambridge University Press, Cambridge, 1997; paperback ed. 2005).

⁶O. Qasaimeh, W.-D. Zhou, J. Phillips, S. Krishna, P. Bhattacharya, and M. Dutta, *Appl. Phys. Lett.* **74**, 1654 (1999).

⁷H. D. Summers, D. R. Matthews, P. M. Smowton, P. Rees, and M. Hopkinson, *J. Appl. Phys.* **95**, 1036 (2004).

⁸J. P. Tourrenc, S. O'Donoghue, S. Hegarty, M. Flynn, G. Huyet, J. McInerney, L. O'Faolain, and T. F. Krauss, *IEEE Photonics Technol. Lett.* **18**, 2317 (2006).

⁹E. A. Viktorov, P. Mandel, I. O'Driscoll, O. Carroll, G. Huyet, J. Houlihan, and Y. Tanguy, *Opt. Lett.* **31**, 2302 (2006).

¹⁰Y. Tanguy, J. Houlihan, G. Huyet, E. A. Viktorov, and P. Mandel, *Phys. Rev. Lett.* **96**, 053902 (2006).

¹¹A. Markus and A. Fiore, *Phys. Status Solidi A* **201**, 338 (2004).

¹²K. Mukai, N. Ohtsuka, and M. Sugawara, *Jpn. J. Appl. Phys., Part 2* **35**, L262 (1996).

¹³A. Markus, M. Rossetti, V. Calligari, D. Chek-AI-Kar, J. X. Chen, A. Fiore, and R. Scollo, *J. Appl. Phys.* **100**, 113104 (2006).